Palaeogeography, Palaeoclimatology, Palaeoecology 268 (2008) 47–57

Contents lists available at ScienceDirect

Palaeogeography, Palaeoclimatology, Palaeoecology

journal homepage: www.elsevier.com/locate/palaeo

# A new magnetostratigraphic framework for late Neogene *Hipparion* Red Clay in the eastern Loess Plateau of China

Yanming Zhu [a], Liping Zhou [a,*], Duowen Mo [a], Anu Kaakinen [b], Zhaoqun Zhang [c], Mikael Fortelius [b,d]

[a] Laboratory for Earth Surface Processes, Department of Geography, Peking University, Beijing 100871, China
[b] Department of Geology, P.O. Box 64 (Gustaf Hällströmin katu 2a) FIN-00014 University of Helsinki, Finland
[c] Institute of Vertebrate Paleontology and Paleoanthropology, Chinese Academy of Sciences, Beijing 100044, China
[d] Institute of Biotechnology, P.O. Box 56, FIN-00014 University of Helsinki, Finland

ARTICLE INFO

*Article history:*
Received 1 May 2008
Received in revised form 2 August 2008
Accepted 5 August 2008

*Keywords:*
China
Magnetostratigraphy
Late Neogene
Red Clay

ABSTRACT

Mammalian fossils, especially the *Hipparion* fauna, found in the Red Clay of the Loess Plateau, are of immense value for reconstructing late Neogene paleoecology and paleoclimatology in northern China. The lack of a precise chronological framework for these fossil sites has impeded our understanding of the evolution of the Chinese mammalian fauna, their correlation with European mammalian units, and the retrieval of paleoclimatic information. In this study, a field survey of regional stratigraphy in the Baode area of Shanxi was carried out and three profiles (Tanyugou, Yangjiagou-I and Yangjiagou-II) of Late Neogene deposits were selected for detailed investigation. A new chronological framework of the Late Neogene sequences in the Baode area is established by means of paleomagnetism. Our results show that the Red Clay accumulation in the Baode area began at least 7.23 Ma ago. Deposition continued to the superposed Jingle Formation. The most continuous and complete exposure of the Jingle Formation known to date was identified and dated to 2.72~5.34 Ma. A lithological distinction between the Jingle Formation and the underlying Baode Formation forms a clear boundary in the Red Clay that is not coincident with the Miocene/Pliocene boundary documented elsewhere. Three rich fossil layers are found in the Yangjiagou-II profile and dated to 6.43–6.54 Ma, 6.83–6.86 Ma and 7.15–7.18 Ma, respectively. With the application of three different demagnetization techniques, the Matuyama–Gauss geomagnetic reversal boundary was identified in a transitional unit between loess and typical Red Clay deposits. A lock-in depth of as large as 6.8 m (corresponding to ca. 65 ka) was inferred but remains unexplained.


## 1. Introduction

Continuous late Cenozoic aeolian deposits are widely distributed in the Loess Plateau of China (Liu, 1985). Spatially, the Loess Plateau can be divided into northern, southern, western, eastern and central parts, each with characteristic thicknesses of aeolian sequences depending on local geomorphological and climatic conditions. Lithostratigraphically, the aeolian sequences can be broadly divided into two major units: the upper Quaternary loess–paleosol sequence and the lower Miocene–Pliocene red earth. With the recent discovery of aeolian sequences back to 22 Ma, the Miocene–Pliocene red earth can be further divided into Late Miocene–Pliocene Red Clay and the Miocene loess (Guo et al., 2002). The upper loess–paleosol sequences have been intensively studied for reconstructing the Quaternary paleoclimate history in northern China (Heller and Liu, 1982, 1986; Liu, 1985; Liu and Ding, 1990; Zhou et al., 1990; An et al., 1990, 1991; Rutter et al., 1991; Hus and Han, 1992; Liu and Ding, 1998). The underlying Red Clay sequence was first described as *Hipparion* red earth due to the wide occurrence of hipparionine horses in the deposits (Anderson, 1923; Zdansky, 1923; Jokela et al., 2005). It started to attract international attention immediately after the report of the extremely rich mammalian faunas in the 1920's (e.g., Anderson, 1923; Zdansky, 1923; Sefve, 1927), and was the subject of intensive taxonomic research in the following decades. The results of this early work were synthesised by Kurtén (1952).

For a long time, the chronology of the Red Clay sequence was based on isolated local fossil faunas according to their evolutionary stages. With the introduction of magnetostratigraphy to the late Neogene sequences in northern China since the 1980s, new chronological framework for a series of Red Clay sequences has been established mainly in the central and southern part of Loess Plateau (Liu et al., 1988; Evans et al., 1991; Zheng et al., 1992; Sun et al., 1998; Ding et al., 1998a, 1998b; Qiang et al., 2001). Magnetic susceptibility, grain size, geochemical and lithologic properties, and micromorphology of the Red Clay sequences have been extensively examined under the new chronological framework, and have yielded valuable information on the paleoclimatic variability of northern China and the Asian monsoon evolution. This has also allowed investigation of the link between aeolian deposition in Asia and the growth of the Tibetan Plateau and

* Corresponding author. Tel.: +86 10 62756052; fax: +86 10 62754411.
*E-mail address:* lpzhou@pku.edu.cn (L. Zhou).

0031-0182/$ – see front matter © 2008 Elsevier B.V. All rights reserved.
doi:10.1016/j.palaeo.2008.08.001

global cooling since the Late Neogene (Liu et al., 1988; Evans et al., 1991; Zheng et al., 1992; Sun et al., 1998; Ding et al., 1998a,b; Dodonov & Zhou, 2008).

In addition to the indirect paleoclimatic proxies mentioned above, paleobiologic records such as mammalian fossils and pollen are important sources of information for paleoclimatic reconstruction. Investigations on terrestrial mammal communities and environmental change have been carried out recently in the late Neogene deposits in the central and southern parts of Loess Plateau (Xue et al., 1995, 2006; Zhang et al., 1997, 2001, 2002; Wang and Deng, 2005; Wang et al., 2006; Wu et al., 2006; Zhang, 2006). As the faunal and floral remains preserve information on past environmental conditions in more direct way, their characteristics can be taken as sensitive indicators of past climate (Shi et al., 1993; Fortelius et al., 2002).

However, in contrast to the extensive and detailed investigations of the aeolian sequences in the central and southern part of Loess Plateau, little work has been done to the late Neogene aeolian deposits in the eastern Loess Plateau (Mo and Derbyshire, 1991; Zhang et al., 1995; Qiang et al., 2001; Han et al., 2002; Deng et al., 2004; Yue et al., 2004). For historical reasons, the aeolian sequences in the Baode area of Shanxi in the eastern Loess Plateau are special in the study of the Chinese Neogene stratigraphy. Baode is one of the most representative areas where the typical *Hipparion* fauna was first discovered and the Baode Red Clay was defined (Zdansky, 1923; Teilhard and Young, 1930, 1931). Although numerous studies have been made on the fossils, laying the foundation of Late Neogene mammalogy in China (Zdansky, 1923; Teilhard and Young, 1930, 1931; Pei et al., 1963; Liu et al., 1978; Li et al., 1984; Qiu et al., 1987; Qiu, 1988), systemic investigation on chronology in this area has been surprisingly sparse (Deng et al., 2004; Yue et al., 2004). Due to the lack of precise age controls on the fossil-bearing beds and the isolated occurrence of fossils at different localities, the retrieval of paleoenvironmental information from mammalian fossils has been greatly limited. This also makes it difficult to correlate the rich mammalian fauna assemblages of the Baode area with those of other areas, hence impeding the establishment of an accurate chronology for the evolution of Neogene land mammalian in China.

In this study, we undertook a field survey of the regional stratigraphy in the Baode area and investigated three profiles of Late Neogene deposits. Based on detailed paleomagnetic measurements, a new chronological framework for the Late Neogene *Hipparion* Red Clay sequences in the Baode area is established. When integrated with previous studies in other areas, this will help to improve the chronology of the mammalian fossils found in this area especially for the classic localities, and will facilitate a regional correlation with respect to Neogene mammal evolution and paleoenvironment.

## 2. Geological setting

### 2.1. Regional lithostratigraphy

The Baode area is located in the northeastern part of the Loess Plateau in the northern part of Shanxi Province. It is flanked to the east by the Luliang Mountains and to the west by the Yellow River (Fig. 1). During the late Cenozoic Era, terrestrial clastic sediments have been deposited in most parts of this area. The landforms of this area are dominated by undulating bedrock capped by late Cenozoic loess and Red Clay deposits, which are dissected into a complex network of steeply sloping gullies and valleys.

The earliest stratigraphic scheme of the late Neogene strata in this area was established by Zdansky in 1923. Later, two units (i.e. Baode Formation and the Jingle Formation) were defined by Teilhard and Young (1930, 1931). Since then, few studies have been carried out to refine the scheme. Our field investigation in this area was mainly focused on the deposits of Late Neogene age. Ten sedimentary profiles along the east-west-trending gullies in this area were logged and measured in detail to establish the stratigraphical framework and distribution of the sedimentary facies (Fig. 2).

The Baode Formation is about 100-m thick and rests on the pre-Cenozoic basement with an angular unconformity. It contains rich mammalian fossils which were assigned a Late Miocene age (Li et al., 1984). The sedimentary sequences at Yuejiagou, Jijiagou, Daijiagou, Junchi, Qiaotou and Yangjiagou (Fig. 1b) yielded large numbers of mammalian fossils. Among them, Yuejiagou, Jijiagou and Daijiagou were the places where the classic mammalian fossil localities of Zdansky (1923) were found (Fig. 2).

According to the lithological characteristics, the Baode Formation can be divided into two parts. The lower part can be observed in Junchi, Qiaotou, Tanyugou and Luzigou and comprises a ca. 25-m unit of conglomerate beds with interbedded gray marl. It was originally defined as the Luzigou Formation and was separated from the overlying *Hipparion* red earth, and considered to be of Miocene age (Zdansky, 1923). However, Teilhard and Young (1930, 1931) considered that it should be synchronous with the *Hipparion* red earth and the age should be of early Pliocene, as then conceived, according to the mammalian fossils. The upper part, which can be seen clearly in Tanyugou and Yangjiagou, is made up of a 75-m thick sequence of red brown clay with carbonate nodule horizons, gravel layers and silt-silty clays with horizontal bedding.

The overlying Jingle Formation is about 40 m thick and characterized by dark reddish clay intercalated with carbonate horizons and with abundant Fe–Mn-coatings. For most of the outcrops, such as at

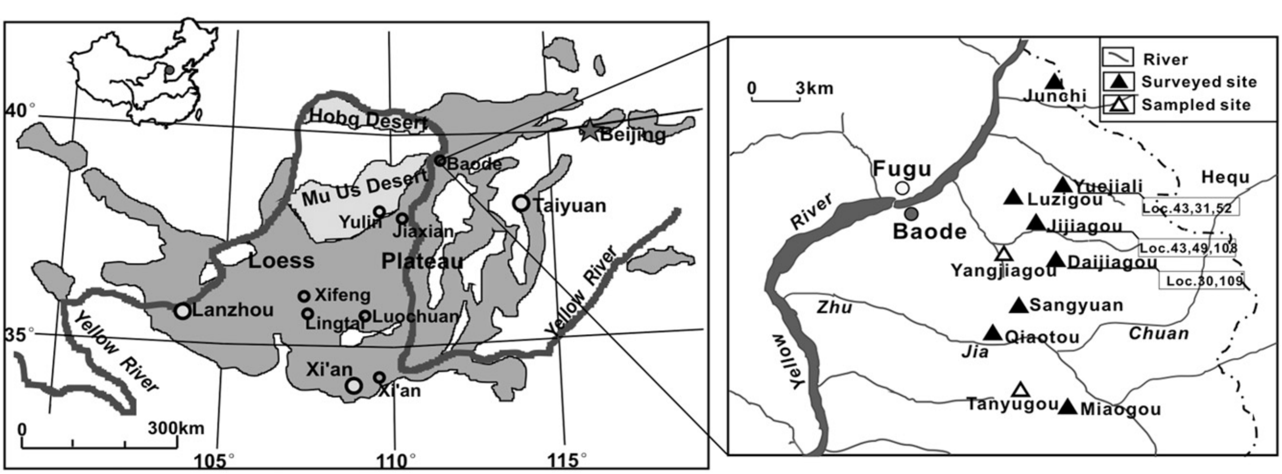


**Fig. 1.** Map showing the distribution of loess and Red Clay deposits and locations of this study (small closed circle) and other loess sections (small open circle) of Loess Plateau (Left), and the locations of surveyed (closed triangle) and sampled (open triangle) sites in the study area (Right).

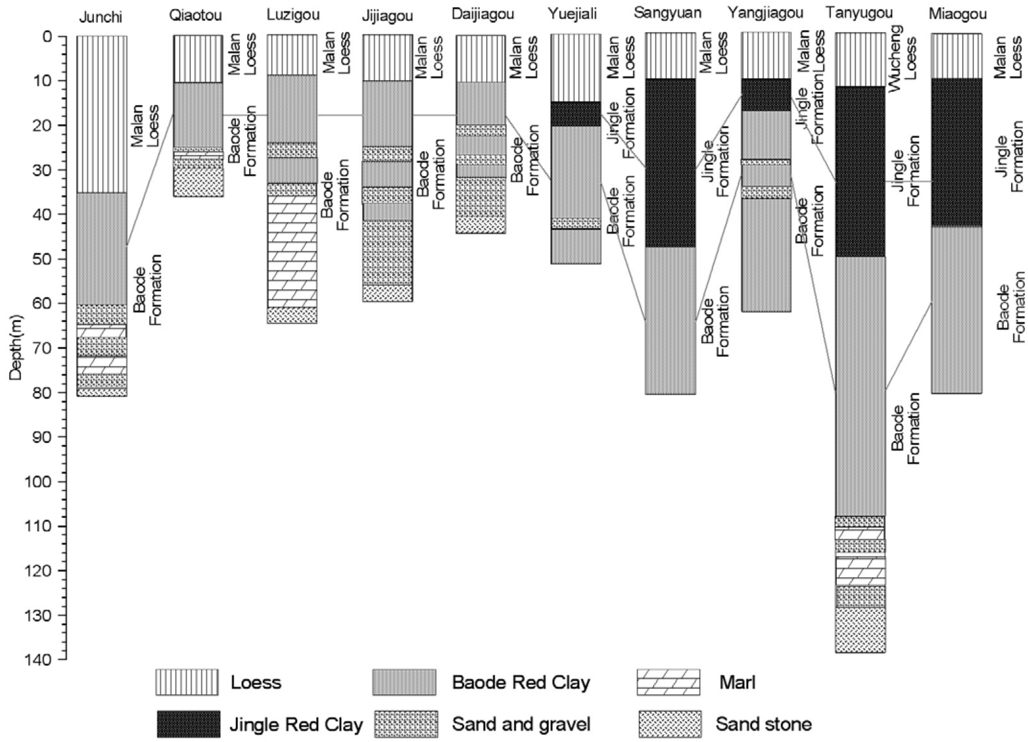


**Fig. 2.** Ten profiles logged and their stratigraphic correlation in Baode area.

Yangjiagou and Miaogou, only the lower part of Jingle Formation is present. The complete Jingle Formation is rarely seen and has been found only in Sangyuan and Tanyugou, while continuous deposits with the lower part of the overlying Wucheng Loess are exposed only at Tanyugou.

### 2.2. Lithostratigraphy of three working profiles

After detailed field survey, we chose the Tanyugou, Yangjiagou-I and Yangjiagou-II profiles as our working profiles. The Tanyugou profile provides the best opportunity for a continuous sedimentological and stratigraphical study of the lower part of Wucheng Loess, the Jingle Formation and the upper part of Baode Formation. The Yangjiagou-I and Yangjiagou-II profiles were chosen for the occurrence of rich and diversified mammal fossils.

The Tanyugou profile is located about 20 km to the south of the town of Baode (Fig. 1). This profile is 140 m thick, and we sampled the top 90.5 m for this study (Fig. 3). The top 13.6 m corresponds to the lowest part of Wucheng Loess, which is intercalated with reddish brown paleosols. Carbonate nodule layers generally occur beneath the paleosols. Six loess–paleosol layers can be recognized from the top to the bottom as $S_{30}$, $L_{31}$, $S_{31}$, $L_{32}$, $S_{32}$ and $L_{33}$. The coarse-grained sandy loess $L_{33}$, which occurs at the depth of 9.2 m to 13.6 m, is a marker layer pinpointing the bottom of the Wucheng Loess. The lower part of Tanyugou profile, reddish and 70.9-m in thickness, is the Jingle Formation and the upper part of the Baode Formation. A transitional unit (TU) is identified in the measured section between the Wucheng Loess and Jingle Formation (between 13.6 m to 19.6 m) where the colour changes gradually downwards from yellow to reddish. Soils are weakly developed compared to those of the underlying Red Clay.

The Jingle Formation is about 40.9 m thick, and consists of dark Red Clay with remarkably strong pedogenesis indicated by its colour and soil structure. According to field observations, the Jingle Formation can be lithologically divided into two units. The first unit extends from 19.6 m to 41 m. Soils within this unit are the most strongly developed throughout this profile with abundant clay and Fe–Mn coatings. The second unit from 41 m to 60.5 m contains relatively weakly developed soils compared to the overlying unit with less clay content and Fe–Mn coatings.

The upper 30 m of the Baode Formation is characterized by a dominance of reddish to brownish clays interbedded with carbonate horizons. The fine-grained deposits are mainly structureless and commonly contain pedogenic features in varying amounts. The coarser lithofacies are restricted to thin lenticular or sheet-like bodies of coarse silts and granule–pebble conglomerates. Based on field observations, the upper part of the Baode Formation can be subdivided into three units. The first unit extends from 60.5 m downwards to 73.6 m. Pedogenesis is relatively weak with a generally brownish color. The base of the unit is marked by a 1-m-thick bed of horizontally laminated silty clay. The second unit ranges from 73.6 m to 85.7 m and is characterised by more reddish and more strongly developed soil layers than the first unit. The third unit extends from 85.7 m to 90.5 m. Soils within this unit show lighter reddish colour than the second unit.

The Yangjiagou-I and Yangjiagou-II profiles are located near the village of Yangjiagou, about 10 km to the southeast of the town of Baode (Fig. 1). The Yangjiagou-I profile is 43 m thick and consists of the lower part of the Jingle Formation with a thickness of 7 m, and 36-m of the Baode Formation. The Jingle Formation is conformable with the Baode Formation (Fig. 3). The Yangjiagou-II profile lies about 700 m west of the Yangjiagou-I profile. There is a 7-m loess-paleosol at the top of the Yangjiagou-II section. It lies in angular unconformity with the Baode Formation, which is 56 m in thickness and contains three fossiliferous horizons at the depth of 26.0–28.6 m, 43.2–44.6 m and 58.5–59.9 m, respectively (Fig. 3).

The two Yangjiagou profiles can be correlated by tracing the marker layers along the gully. The layers at 21.7–32.5 m and 32.5–42.4 m in Yangjiagou-I profile can be correlated with the layers at 5.6–19.8 m and 19.8–28.2 m in the Yangjiagou-II profile, respectively (Fig. 3). Lithostratigraphic correlation can also be made between the Tanyugou profile and the Yangjiagou-I profile. Since the Jingle

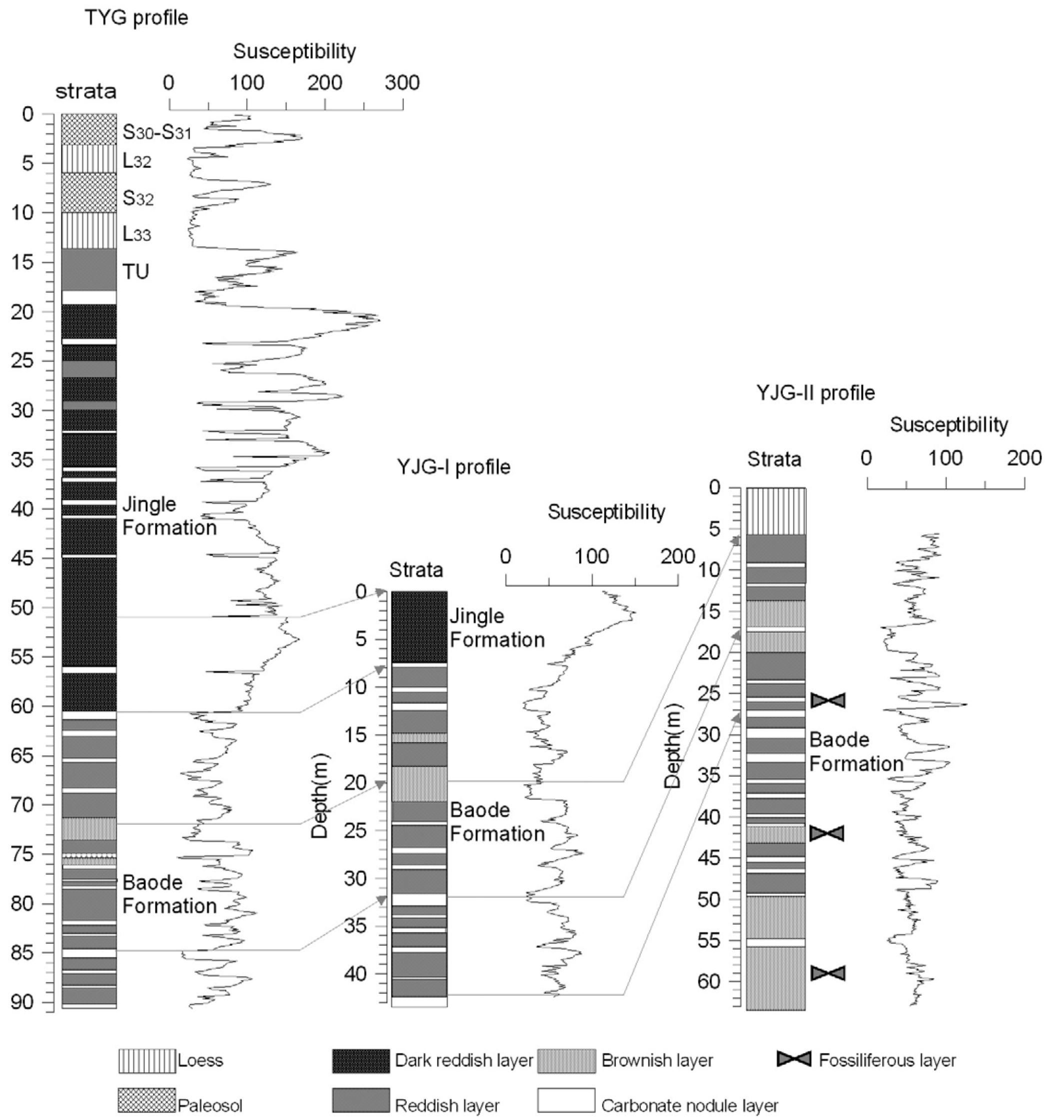


**Fig. 3.** Lithological column and magnetic susceptibility curves of the three measured profiles.

Formation and the Baode Formation of these two profiles are in conformable contact, the boundary between the Jingle and Baode Formations can be used as a marker horizon to aid stratigraphic correlation. The top 7.7 m of the Jingle Formation at the Yangjiagou-I profile can be correlated with a layer at 50–60.5 m at the Tanyugou profile. In addition, layers at 7.7–21.7 m and 21.7–32.5 m at the Yangjiagou-I profile can be correlated with the layers at 60.5–73.6 m and 73.6–85.7 m at the Tanyugou profile, respectively (Fig. 3). All the correlations based on detailed field observations are further verified by patterns of magnetic susceptibility variations (Fig. 3).

## 3. Sampling, sample preparation and experimental methods

Samples were taken from the three profiles for magnetic susceptibility measurements. Low field magnetic susceptibility and frequency-dependent magnetic susceptibility were measured using a Bartington MS2B magnetic susceptibility meter at the Quaternary Environmental Magnetism Laboratory of Peking University.

A total of 2713 powder samples were collected at an interval of 5 cm for the upper part (0–25 m) of Tanyugou profile and 10 cm spacing for the lower part of Tanyugou profile and for the other two profiles. In addition, 270 oriented block samples were collected at an interval of 20 cm along the Tanyugou profile and 624 oriented block samples were collected at an interval of 10 cm along the Yangjiagou-I and Yangjiagou-II profiles.

Oriented block samples were cut into 2 cm cubic specimens for paleomagnetic measurements. One cubic specimen of each sample was subjected to thermal demagnetization using a 20–50 °C increment from room temperature to 585 or 680 °C with a MMTD80 Thermal Demagnetizer. Remanent magnetization was measured using a 2G cryogenic magnetometer at the Paleomagnetism Laboratory of the Institute of Geology and Geophysical, Chinese Academy of Sciences. Both the demagnetizer and magnetometer were housed in a field-free space (<300 nT) to avoid contamination by viscous magnetization.

Since some earlier studies (Qiang et al., 2001; Spassov et al., 2001) have noted that directional patterns of the characteristic remanent magnetization (ChRM) may be sensitive to different demagnetization techniques, the other two sets of parallel cubic specimens around the Matuyama/Gauss boundary (MGB), at the depth of between 14.0 to 16.8 m at the Tanyugou profile, were selected for an experiment with two additional demagnetization approaches. One set of the samples was subjected to alternating field (AF) demagnetization with peak filed values of 5, 10, 20, 25, 30, 35, 40, 45, 50, 60, 80, and 100 mT. Another set of the samples was first thermally demagnetized by steps of 50 °C from room temperature to 150 °C, then further demagnetized

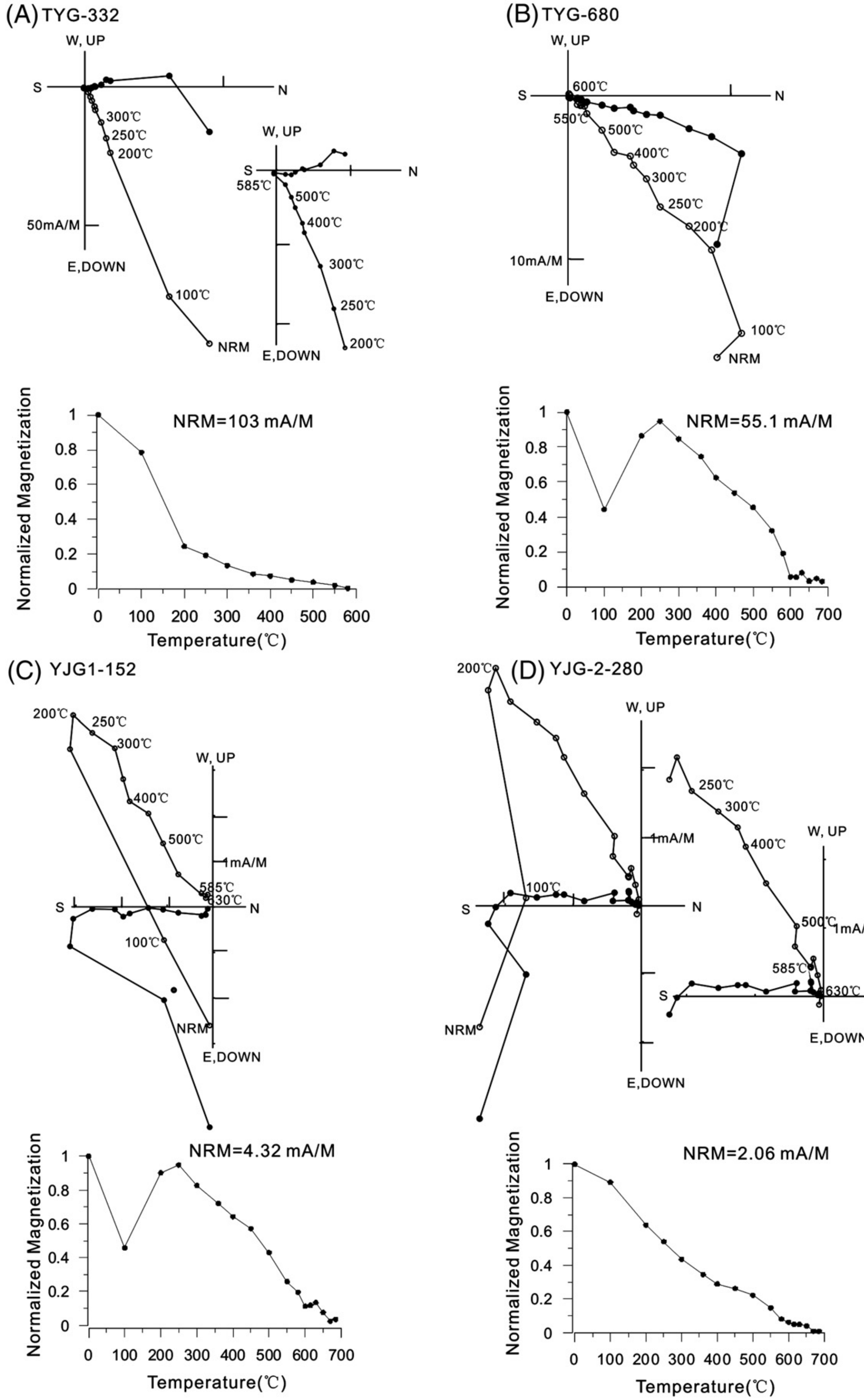


**Fig. 4.** Orthogonal projections of NRM vector and the NRM intensity of typical samples. Solid (open) symbols refer to the projection on the horizontal (vertical) plane in geographic coordinates.

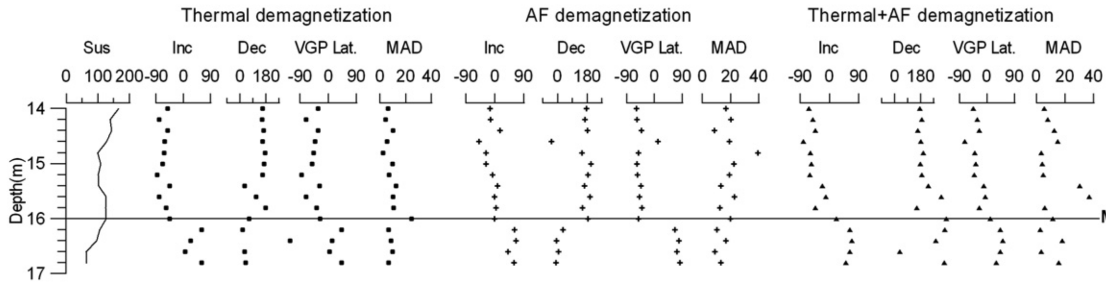


**Fig. 5.** Directional behavior of the Matuyama/Gauss Boundary transitional polarity interval in the Tanyugou profile for three different demagnetization techniques.

by AF method with peak filed values of 5, 10, 20, 25, 30, 35, 40, 45, 50, 60, 80 and 100 mT.

## 4. Results

### 4.1. Magnetic susceptibility

Variations in susceptibility from the three profiles show a strong correlation with the degree of soil development and are consistent with field observations (Fig. 3). In general, magnetic susceptibility values are higher in paleosols than in loess for the Wucheng Loess. The magnetic susceptibility of the Red Clay shows patterns different from the overlying loess–paleosol. There is a longer periodicity and an upwards increasing trend compared to the loess–paleosol part. The highest values occur at the Red Clay of the upper part of the Jingle Formation. The lower part of the Jingle Formation has susceptibility values close to those of paleosols in the loess–paleosol succession. The magnetic susceptibility values of the Red Clay of the Baode Formation are lower than that of the Jingle Formation and the overlying paleosols (Fig. 3). The higher values in the Baode Formation coincide with the reddish layers with higher clay content whereas low values typify layers with higher silt content and brownish colour. Magnetic susceptibility curves of these three profiles confirm the stratigraphic subdivision and correlation of the three profiles based on field observations.

### 4.2. Magnetostratigraphy

Typical thermal demagnetization diagrams for normal and reversed samples are shown in Fig. 4. All the samples show the presence of two components. A secondary component of the natural remanent magnetization is removed by thermal treatment in the interval 200–300°C (Fig. 4). The direction of this component is consistent with the present day field and is a viscous overprint. Upon removal of the low temperature component, the direction becomes relatively stable and the vector decays towards the origin on the Zidjerveld orthogonal plot. According to Zhou and Shackleton (1999), this direction is interpreted as the primary magnetization acquired *after* deposition (see discussion below). The unblocking temperatures at and above 580 °C (Fig. 4b, c, d) indicate contributions of both magnetite and hematite to the remanent magnetization. The directions of the primary component were calculated using principal component analysis (Kirschvink, 1980) and analyzed using standard Fisher statistics (Fisher, 1953).

Fig. 5 gives the experimental results of sensitivity test for three different demagnetization techniques. It shows that the three methods

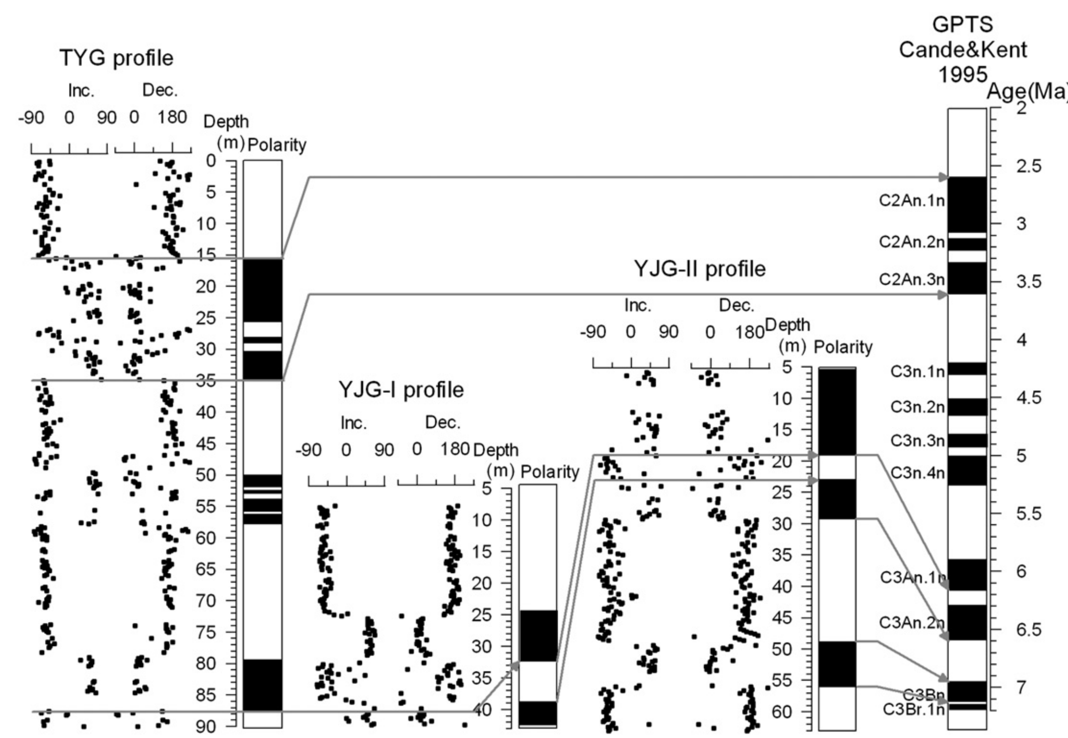


**Fig. 6.** Magnetostratigraphy of TYG, YJG-I and YJG-II profiles, compared with the Geomagnetic Polarity Time Scale of Cande and Kent (1995). Black parts are normal polarity, and white parts are reversed polarity.

**Table 1**
The depth and age of the reference points

| The age reference point | Depth (m) | Age (Ma) | Data source |
|---|---|---|---|
| Base of $S_{30}$ | 0.6 | 2.24 | Heslop et al., 2000 |
| Top of $S_{31}$ | 1.5 | 2.341 | |
| Base of $S_{31}$ | 3 | 2.369 | |
| Top of $S_{32}$ | 6.6 | 2.54 | |
| Base of $S_{32}$ | 9.2 | 2.596 | |
| Base of $L_{33}$ | 13.6 | 2.62 | |
| Top of Red Clay | 19.6 | 2.72 | Sun et al., 2006 |
| Kaena (T) | 25.6 | 3.045 | Lisieki and Raymo, 2005 |
| Kaena (B) | 28 | 3.127 | |
| Mammoth (T) | 28.8 | 3.21 | |
| Mammoth (B) | 30.2 | 3.319 | |
| Gauss/Gilbert | 34.8 | 3.588 | |
| Cochiti (T) | 48.8 | 4.184 | |
| Cochiti (T) | 52 | 4.306 | |
| Nunivak (T) | 52.8 | 4.478 | |
| Nunivak (T) | 53 | 4.642 | |
| Sidufjall (T) | 53.8 | 4.807 | |
| Sidufjall (T) | 55.6 | 4.898 | |
| Thvera (T) | 56 | 4.989 | |
| Thvera (B) | 57.8 | 5.254 | |
| C3An.1n (T) | 78.2 | 5.894 | Cande and Kent, 1995 |
| C3An.1n (B) | 87.6 | 6.137 | |
| C3An.2n (T) | 91.0 | 6.296 | |
| C3An.2n (B) | 97.4 | 6.567 | |
| C3An.3n (T) | 116.8 | 6.935 | |
| C3An.3n (B) | 124.0 | 7.091 | |

yield almost the same MGB position in the Tanyugou profile. This result differs from the observations by Spassov et al. (2001) that the directional patterns of the ChRM in two Matuyama/Brunhes geomagnetic polarity boundary transitional records are inconsistent and even dependent on specific demagnetization techniques used. The cause for this discrepancy needs further investigation. In order to assess the reliability of our three sets of data, the maximum angular deviation (MAD) values are also given in Fig. 5. The thermal demagnetization method and thermal plus AF demagnetization method yield comparatively well-defined characteristic remanent magnetization directions, with MAD values generally below 15°. The ChRM directions of the AF demagnetization are not well-defined with MAD values generally exceeding 15°. This indicates that thermal demagnetization and thermal plus AF demagnetization are more effective than AF demagnetization alone, and hence more suitable for isolating the primary remanent magnetization of loess and Red Clay at least for our study sites.

The lithostratigraphy, inclination and declination of the three profiles are shown in Fig. 6. The magnetostratigraphic patterns of the three profiles correlate well with the geomagnetic polarity time scale of Cande and Kent (1995). For the Tanyugou profile, the Matuyama/Gauss boundary is measured at 16.0 m depth in the transitional unit, about 3.6 m above the top of the typical Red Clay. The Gauss normal polarity chron is obtained between 16 and 35 m and contains two reversed polarity subchrons corresponding to the Kaena and Mammoth subchrons. The Gilbert reversed polarity chron occurs between 35 and 79 m and contains the Cochiti, Nunivak, Sidufjall and Thvera subchrons. Chron 3A.1n is registered between 79 and 85 m. The lowest part between 87.9 and 90.5 m corresponds to the reversed part of Chron 3A. In the Yangjiagou-I profile, the uppermost interval of the reversed polarity above 25.6 m is correlated to the Gilbert chron. The two normal polarity intervals of 25.6–32.8 m and 38.8–42.4 m are equivalent to Chron 3A.1n and Chron 3A.2n, respectively. In the Yangjiagou-II profile, the three normal polarity intervals of 5.6–19.5 m, 25–29.4 m and 49.4–52 m correspond to Chron 3A.1n, Chron 3A.2n and Chron3Bn, respectively. The reversed polarity interval of 29.4–42.4 m is correlated to Chron 3Ar.

Figs. 3 and 6 show that the three profiles correlate well in terms of lithology, magnetic susceptibility and magnetostratigraphy. Thus, the sequence from 0 to 87.5 m in the Tanyugou profile and that from 19.4 to 63 m in Yangjiagou-II were chosen to construct a composite profile. We combine our measured magnetostratigraphic boundaries with correlation to existing loess and Red Clay stratigraphy in the central Loess Plateau to construct the chronological framework of Baode composite profile. All age tie points used and their corresponding depths are tabulated in Table 1. A detailed comparison of magnetic susceptibility records between our profiles and the Lingtai and Zhaojiachuan profiles, which were studied by Sun et al. (2006), indicates that the deposits below $L_{33}$ (named as $RC_1$) actually correspond to the transitional unit in the Baode profile. Because our composite profile only covers the lowermost part of the Wucheng loess and there is no magnetic polarity reversal recorded in this part, we correlate the loess–paleosol including the transitional unit to the orbital timescales developed by Heslop et al. (2000) and Sun et al. (2006). The timescale for the underlying Red Clay was established by correlating the measured magnetic polarity reversals with the independently dated magnetic polarity chronology. The timescale provided by Cande and Kent (1995) for the ages before 5.254 Ma and the timescale developed by Lisiecki and Raymo (2005) for the younger ages were used. The ages for the intervals between magnetic reversal boundaries were derived by linear interpolation between adjacent magnetostratigraphic control points.

The chronological framework of the Baode composite profile is shown in Fig. 7. The basal age of the composite profile is 7.23 Ma. The boundary between Jingle Formation and Baode Formation is dated to 5.34 Ma. The three fossiliferous layers, found in the Yangjiagou-II profile, are dated to 6.42–6.54 Ma, 6.83–6.86 Ma and 7.15–7.18 Ma, respectively. The chronological framework enables us to calculate sedimentation rate

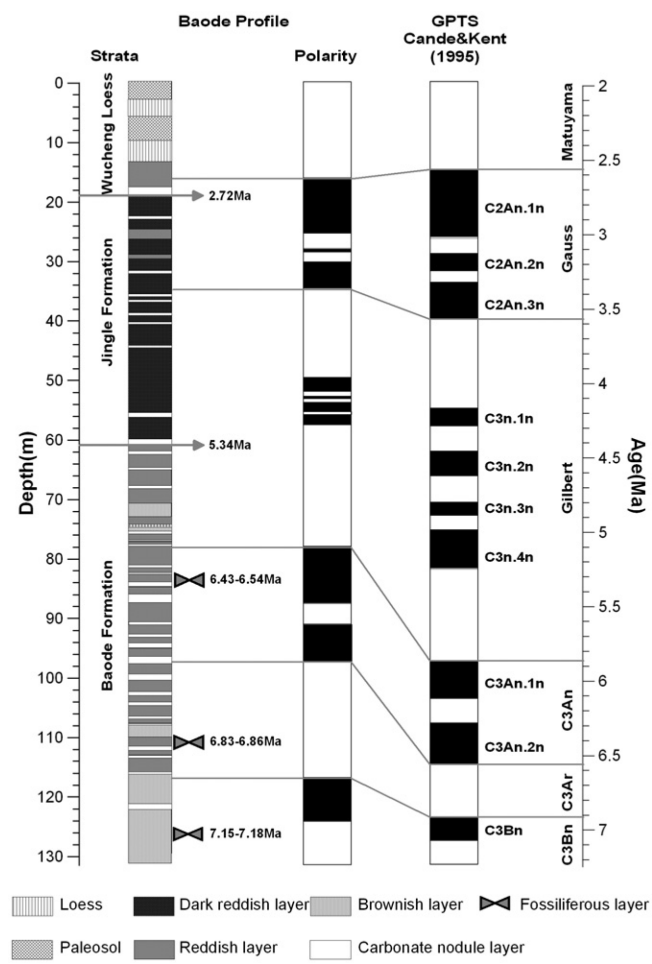


**Fig. 7.** Magnetostratigraphy of the composite profile of Baode, compared with the Geomagnetic Polarity Time Scale of Cande and Kent (1995). Black parts are normal polarity, and white parts are reversed polarity.

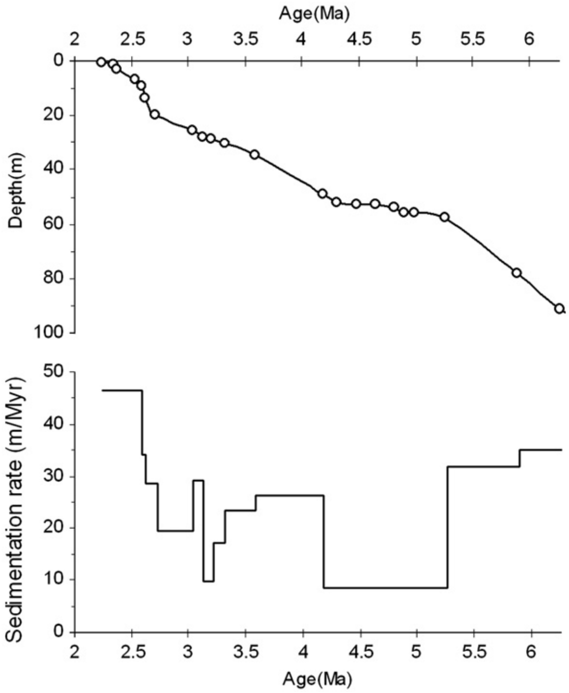


**Fig. 8.** (a) Age-depth plot for the composite profile of Baode, circles are magnetostratigraphic references. (b) Sedimentation rates determined on the basis of the magnetostratigraphy.

for different parts of the Tanyugou profile (Fig. 8). The sedimentation rate decreases from about 34 m/Ma during the interval of 6.26 Ma and 5.25 Ma to about 8 m/Ma between 5.25 Ma and 4.2 Ma. Then it increases to about 26 m/Ma between 4.2 Ma and 3.3 Ma. Afterwards, it gradually increases to a maximum, about 46 m/Ma between 3.2 Ma and 2.2 Ma.

## 5. Discussion

### *5.1. The loess and Red Clay boundary and the Matuyama/Gauss polarity boundary*

In the study of Luochuan loess section, Liu (1985) defined the loess and Red Clay boundary at the base of $W_{L\text{-}3}$ which is one of the most significant stratigraphic markers in the loess sequence and is equivalent to $L_{32}$ at Baoji, Xi'an and Weinan sections (Ding et al., 1990, 1992). Subsequent stratigraphic observations indicate that, in the southern part of the Loess Plateau, another loess–paleosol couplet ($S_{32}$–$L_{33}$) is recognizable below $L_{32}$ (Ding et al., 1992). Accordingly, the bottom of loess unit $L_{33}$ has been regarded as the boundary of loess and Red Clay (Ding et al., 2000, 2002). Detailed stratigraphic observations made by Xue et al. (2001) suggest that there exists a transitional unit (TU) between $L_{33}$ and typical Red Clay, which is ubiquitous across the Loess Plateau. They suggest that the base of the TU should be the boundary between loess and Red Clay. A transitional unit with a thickness of 6 m is also found at Tanyugou profile in this study (Figs. 3 and 9).

Previous paleomagnetic measurements of Lingtai, Baoji, Weinan, Jingchuan, Duanjiapo and Xunyi sections in the central and southern part of Loess Plateau have shown that the MGB is located at different parts of $L_{33}$ (Ding et al., 1998b; Sun et al., 1998; Zhao, 1989; Evans et al., 1991; Yang et al., 2000; Zhu et al., 2000; Xue et al., 2001). Although the MGB at Luochuan and Xifeng sections was found lying in the upper part of the Red Clay (Heller and Liu, 1982, 1986; Sun et al., 1998), both these sections have taken the base of $W_{L\text{-}3}$ ($L_{32}$) as the boundary of loess and Red Clay, and hence the MGB is in fact also located in $L_{33}$ (Ding et al., 1990; An et al., 2000). As mentioned above, the MGB in Baode profile is found in the transitional unit. The only similar observation so far was made at Jiaxian section, which was studied in detail by Ding et al. (1998a) and subsequently by Qiang et al. (2001). Interestingly, this site is also located in the northern part of eastern Loess Plateau. Therefore, it seems that there is a downward displacement of the MGB position along a north-south transect across the Chinese Loess Plateau.

The occurrence of the MGB in loess deposits within $L_{33}$ or the transitional unit would correspond to marine oxygen isotope stage (MIS) 104 with an astronomical age of 2.6 Ma or older (Heslop et al., 2000; Sun et al., 2006). However, the MGB in marine sediments is reported to be at the boundary between MIS 102 and MIS 103 with an astronomical age of 2.58 Ma (Shackleton et al., 1990, 1995). The offset of the MGB recorded in loess-Red Clay sequence and the marine sediments may be caused by the lock-in effect that was discussed by Zhou and Shackleton (1999). If this is the case, the lock-in depth of MGB in the Baode profile is 6.8 m. The MGB within Baode profile is then displaced by about 65 ka, which is much larger than the lock-in effect inferred by Zhou and Shackleton (1999) for the Brunhes–Matuyama boundary at Luochuan. Since the lock-in effect of remanence acquisition in loess deposits is related to the structure of loessic materials and regional climates (Zhou and Shackleton, 1999; Zhou et al., 2000; Nawrocki et al., 2002), the much larger lock-in depth of the MGB in the Baode and Jiaxian sections might be due to the combined effect of coarser grain size of $L_{33}$ and the drier climate compared to that of the sections in the central and southern parts of the Loess Plateau.

### *5.2. The age of Jingle Formation*

The Jingle Red Clay was originally put forward by Teilhard and Young (1930) based on mammalian fossils in Hefeng section, Jingle County, Shanxi Province. Pei et al. (1963) established the Jingle Stage and Jingle Formation without detailed descriptions. No significant progress was made with respect to the chronologic studies until 1994. The magnetostratigraphic work on the Jingle Formation of Hefeng section indicated that its age is 2.5–3.4 Ma (Chen, 1994; Flynn et al., 1997). A different age (2.5–3.0 Ma) for Jingle Formation in the same section was later reported by Yue and Zhang (1998). Subsequently, the Duanjiapo section at Lantian in Shaanxi Province was suggested to be the stratotype section for Jingle Formation, instead of the Hefeng section (Zhang et al., 1999). However, since the lithology of the Lantian sequence at Duanjiapo points to a gradual change in the sedimentological pattern from mainly fluvial to predominantly aeolian Red Clay deposits, without a distinguishable boundary (Zhang et al., 2002; Kaakinen and Lunkka, 2003), it does not satisfy the basic requirement for a stratotype. In a more recent magnetostratigraphic study by Yue et al. (2004), the sequence investigated in the Baode area did not cover the uppermost part of Jingle Formation and the lowermost Baode Formation. Currently, there is no agreement on the basal age of the Jingle Formation. While Yue et al. (2004) place it at 5.3 Ma, Zhang and Liu (2005) correlate the Jingle Formation to the Chinese mammalian Biozone 6 and the European Mammal Neogene unit 16 (MN16), hence with a basal age of 3.2 Ma between Chrons C2An.2r and C2An.2n (Agusti et al., 2001). This is consistent with that of Flynn and Wu (2001) who posit MN16 for Jingle correlative, Mazegou Formation.

Therefore, a complete and continuous sequence of Jingle Red Clay has been needed to resolve the age problem of the Jingle Formation. According to the original definition by Theihard and Young (1930), the Jingle Stage represents the deposits formed in the Pliocene. Note that the Early Pliocene for these authors was considered as late Miocene now. Nevertheless, due to the lack of a complete sequence of the Jingle Formation, the Jingle stage was replaced by the Gaozhuangian stage (Qiu and Qiu, 1990). The Jingle Red Clay found at Tanyugou in this study represents the most complete typical deposits of Jingle stage. Based on our magnetostratigraphic timescale, the age of the Jingle Formation is in the range between 5.34 Ma and 2.72 Ma. The Baode/Jingle boundary marks a clear sedimentological divide which does not coincide with the boundary between Miocene and Pliocene at 5.23 Ma established in the marine sediments.

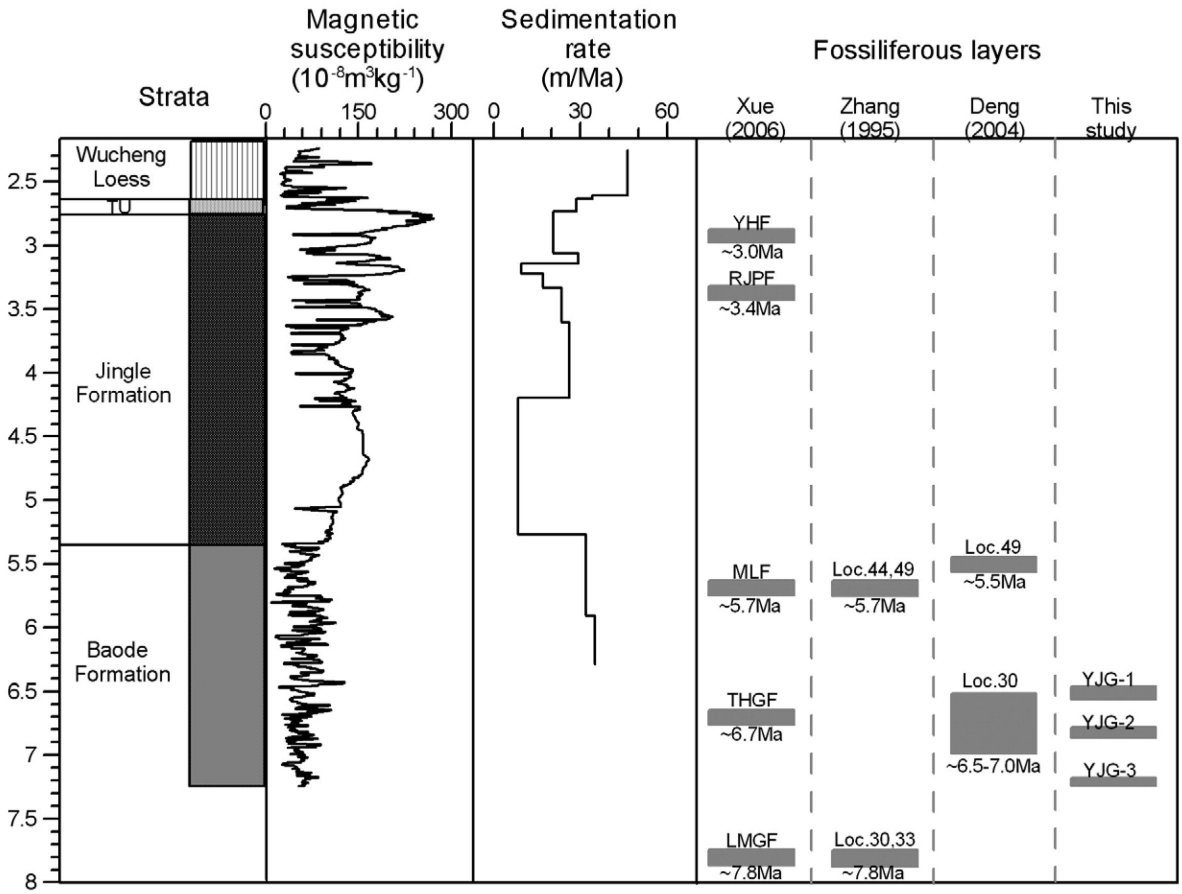


**Fig. 9.** Lithostratigraphy, magnetic susceptibility, sedimentation rate of the composite profile of Baode and projected ages for fossiliferous faunas of Baode and other areas in the Loess Plateau. TU (the transitional unit between the Loess and Red Clay). YHF (Youhe Fauna), RJPF (Renjiapo Fauna), MLF (Miaoliang Fauna), THGF (Taohuagou Fauna), LMGF (Lamagou Fauna), YJG-1 (the upper fossiliferous layer of YJG-II profile), YJG-2 (the middle fossiliferous layer of YJG-II profile), YJG-3 (the lower fossiliferous layer of YJG-II profile).

### *5.3. A new chronological framework for the Hipparion Red Clay and its implications for the age of old mammalian localities at Baode*

The magnetostratigraphic investigation for the *Hipparion* Red Clay in the Baode area was carried out by Yue et al. (2004) on a Red Clay sequence at Jijiagou with a thickness of 44.1 m. The Jingle Formation and the Baode Formation in this profile have thicknesses of about 14.4 m and 29.7 m respectively, and the corresponding age ranges are 3.0–5.3 Ma and 5.3–8.0 Ma. Our sedimentological and magnetostratigraphic work, with higher resolution on the continuous sequence from the lower part of Wucheng Loess, through Jingle Formation to the middle part of Baode Formation in the three representative profiles provides a new and more detailed chronological framework for the *Hipparion* Red Clay in Baode area. Our estimation for the base of the Jingle Formation is similar to that of Yue et al. (2004), but the more complete succession of Jingle Red Clay allows us to arrive a more accurate age for the upper boundary of the Jingle Formation. Unfortunately, the bottom age of the Baode Formation is still not determined. However, about 70 m sediments of the lower part of the Baode Formation has been found in Tanyugou in our recent field investigation. Further magnetostratigraphic work on this unit has the potential to obtain a definitive age for the base of the Baode Formation.

Many mammalian fossils were reported in the late Neogene Red Clay from different old localities in the Baode area (Zdansky, 1923). The ages of all the mammalian fossils have been considered to be broadly Late Miocene according to mammalian biochronology in the earlier studies (Zdansky, 1924; Teilhard and Young, 1931; Kurtén, 1952; Forsten, 1985; Qiu et al., 1987; Bernor et al., 1990). This has made the correlation of the Chinese late Neogene land mammals with those of western Eurasia very difficult, hence impeding our understanding of the precise evolutionary stages of different mammalian assemblages.

By correlating the mammalian assemblages from Loc.30, 31 and Loc.49, 44 with those from Lamagou and Miaoliang of Fugu, Shaanxi Province respectively, Zhang et al. (1995) obtained an age of about 5.3 Ma for Loc.49, 44 and an age of about 7.4 Ma for Loc.30, 31 (Fig. 9). Xue et al. (2006) made older estimates, with the age of Miaoliang fauna about 5.7 Ma and the age of Lamagou mammalian fauna about 7.8 Ma. Hence the age of Loc.49, 44 should to be about 5.7 Ma and the age of Loc.30, 31 should be about 7.8 Ma (Fig. 9). However, Deng et al. (2004) obtained different ages for Loc.30 and Loc.49 based on the magnetostratigaphic work at Jijiagou section in Baode. They suggested that the age of Loc.49 is about 5.5 Ma and the age of Loc.30 is 6.5–7 Ma (Fig. 9). However, the detailed map published by Zdansky (1923, Plate V) shows that Loc. 49 is at the base of the Red Clay, while Loc. 30 is near the top. These relative positions were confirmed by us during recent fieldwork in the area. Clearly, the precise age assignments of the other old mammalian localities as well as their correlation with other regions such as Yushe Basin (e.g. Tedford et al., 1991; Flynn et al., 1997) remain a challenge ahead.

### *5.4. Potential value for paleoclimatic reconstruction*

Fig. 9 presents variations in magnetic susceptibility and sedimentation rate for the major lithostratigraphical units and a summary of current age assignments for the mammalian fauna of Baode area and the mammalian fossils found in other areas. Three features are striking, i.e. the difference in the magnetic susceptibility and sedimentation rate between the Late Miocene and the Pliocene, the paucity of mammalian fossil finds within the Jingle Formation, and the significant difference in the assigned age for the same classic mammalian fossil localities.

Three distinct stages may be recognized on the basis of the physical properties of the strata. The first interval covers ~7.23 to ~5.3 Ma. Here magnetic susceptibility changes with relatively lower amplitude but higher frequency. It contains relatively thick carbonate nodule horizons and displays a relatively high sedimentation rate. The second interval is from ~5.3 to ~4.2 Ma, and is characterized by the lowest sedimentation rate and consistently higher susceptibility. The third interval is between ~4.2 and ~2.72 Ma, during which the magnetic susceptibility increases gradually (though with large-amplitude fluctuations), accompanied by a concurrent increase in sedimentation rate. Given the complicated nature of magnetic susceptibility in the Red Clay, paleoclimatic interpretation of magnetic signals should await more detailed information on the origin and significance of magnetic properties (An et al., 2001; Ding et al., 2001; Liu et al., 2001).

Fig. 9 also illustrates the potential of the new stratigraphical framework for paleoclimatic reconstruction. The well-constrained three fossil layers from Yangjiagou-II in our study provide new opportunity to clarify the chronological order for the isolated fossil sites. Together with previous investigations, the chronological framework established in our study will provide good reference for future joint efforts involving sedimentology, magnetostratigraphy and mammalian paleontology on the strata of the old isolated localities.

## 6. Conclusions

(1) Based on field investigations and paleomagnetic measurements of three profiles in Baode, Shanxi Province, China, we have obtained a new magnetostratigraphic scheme for the Late Neogene strata and composite chronostratigraphic framework in the Baode area. The basal age of the Baode profile is dated to 7.23 Ma. The three fossiliferous layers found in the Baode profiles correspond to 6.43–6.54 Ma, 6.83–6.86 Ma and 7.15–7.18 Ma, respectively. A systematic study of these well-constrained fossil layers will facilitate a critical evaluation of the isochroneity and diachroneity of mammal fossils across the loess region of northern China.

(2) There exists a transitional unit between loess and typical Red Clay deposits. The Matuyama–Gauss geomagnetic reversal boundary in the Baode profile falls within this unit. The lock-in depth of the Matuyama–Gauss boundary at Baode is estimated to be 6.8 m, corresponding to a displacement of ca. 65 ka, which is significantly larger than that proposed by Zhou and Shackleton (1999) for the Brunhes–Matuyama boundary in the central Loess Plateau.

(3) A continuous and complete record of the Jingle Formation was found in the Baode profile. Based on our magnetostratigraphic investigations, the age of the Jingle Formation ranges between 2.72 and 5.34 Ma. This also provides a record for establishing a precise correlation between terrestrial and marine sequences during the Miocene/Pliocene transition.

(4) There is a significant difference in lithological features, sedimentation rate and fossil mammalian assemblages from the late Miocene to the onset of the Quaternary in the Baode area. According to current biochronology, mammalian fossil finds are much rarer within the Jingle Formation than in the underlying Baode Formation. No obvious paleoenvironmental controls for such a contrast have been identified.

## Acknowledgements

We thank Ben Passey of California Institute of Technology for comments and Xu Feng, Li Changjiang, Pan Yonggang, Liu Qiang and Jiang Wenling of Peking University for their help with the sampling in the field. The work was supported by the National Natural Science Foundation of China (grants 40273007, 40773002) and National Geographic Society.

## References

Agusti, J., Cabrera, L., Garcés, M., Krijgsman, W., Oms, O., Parés, J.M., 2001. A calibrated mammal scale for the Neogene of Western Europe. State of the art. Earth-Science Reviews 52, 247–260.

An, Z.S., Liu, T.S., Lu, Y.C., Porter, S.C., Kukla, G., Wu, X.H., Hua, Y.M., 1990. The long-term paleomonsoon variation recorded by the loess-paleosol sequence in central China. Quaternary International 7/8, 91–95.

An, Z.S., Kukla, G., Porter, S.C., Xiao, J.L., 1991. Magnetic susceptibility evidence of monsoon variation on the Loess Plateau of central China during the last 130,000 years. Quaternary Research 36, 29–36.

An, Z.S., Sun, D.H., Cheng, M.Y., Sun, Y.B., Li, L., Cheng, B.Q., 2000. Red clay sequences in Loess plateau and recorded paleoclimate events of the Late Tertiary. Quaternary Sciences 20 (5), 435–446 (in Chinese with English abstract).

An, Z.S., Kutzbach, J.E., Prell, W.L., Porter, S.C., 2001. Evolution of Asian monsoons and phased uplift of the Himalaya–Tibetan plateau since late Miocene times. Nature 411, 62–66.

Anderson, J.G., 1923. Essays on the Cenozoic of Northern China. Geological Survey China Memoir, Series. A (3), 1–152.

Bernor, R.L., Qiu, Z.X., Hayek, L.A.C., 1990. Systematic revision of Chinese Hipparion species described by Sefve, 1927. American Museum Novitates 2984, 1–60.

Cande, S.C., Kent, D.V., 1995. Revised calibration of the geomagnetic polarity time scale for the Late Cretaceous and Cenozoic. Journal of Geophysical Research 100, 6093–6095.

Chen, X.F., 1994. Stratigraphy and large mammals of the "Jinglean" stage, Shanxi, China. Quaternary Sciences 4, 339–353 (in Chinese with English abstract).

Deng, T., Wang, W.M., Yue, L.P., Zhang, Y.X., 2004. New advances in the establishment of the Neogene Baode Stage. Journal of Stratigraphy 28 (1), 41–47 (in Chinese with English abstract).

Ding, Z.L., Liu, T.S., Liu, X.M., Chen, M.Y., An, Z.S., 1990. Thirty-seven climatic cycles in the last 2.5 Ma. Chinese Science Bulletin 34, 1494–1496.

Ding, Z.L., Rutter, N.W., Han, J.T., Liu, T.S., 1992. A coupled environmental system formed at about 2.5 Ma over eastern Asia. Palaeogeography, Palaeoclimatology, Palaoecology 94, 223–243.

Ding, Z.L., Sun, J.M., Liu, T.S., Zhu, R.X., Yang, S.L., Guo, B., 1998a. Wind-blown origin of the Pliocene red clay formation in the central Loess Plateau, China. Earth and Planetary Science Letters 161, 135–143.

Ding, Z.L., Sun, J.M., Yang, S.L., Liu, T.S., 1998b. Preliminary magnetostratigraphy of a thick eolian red clay-loess sequence at Lingtai, the Chinese Loess Plateau. Geophysical Research Letters 25, 1225–1228.

Ding, Z.L., Rutter, N.W., Sun, J.M., 2000. Rearrangement of atmospheric circulation at about 2.6 Ma over northern China: evidence from grain size records of Loess-palaeosol and red clay sequences. Quaternary Science Reviews 19, 547–558.

Ding, Z.L., Yang, S.L., Sun, J.M., Liu, T.S., 2001. Iron geochemistry of the loess and red clay deposits in the Chinese Loess Plateau and implications for long-term Asian monsoon evolution in the last 7.0 Ma. Earth and Planetary Science Letters 185, 99–109.

Ding, Z.L., Derbyshire, E., Yang, S.L., Yu, Z.W., Xiong, S.F., Liu, T.S., 2002. Stacked 2.6-Ma grain size record from the Chinese loess based on five sections and correlation with the deep-sea $\sigma^{18}$O record. Paleoceanography 17. doi:10.1029/2001PA000725.

Dodonov, A.E., Zhou, L.P., 2008. Loess deposition in Asia: its initiation and development before and during the Quaternary. Episodes 31, 222–225.

Evans, M.E., Wang, Y., Rutter, N., Ding, Z.L., 1991. Preliminary magnetostratigraphy of the Red Clay underlying the loess sequence at Baoji, China. Geophysical Research Letters 18, 1409–1412.

Fisher, R.S., 1953. Dispersion on a sphere. Proceedings of the Royal Society of London. Series A 217, 295–305.

Flynn, L., Wu, W.Y., Downs, W.R., 1997. Dating vertebrate microfaunas in the late Neogene record of Northern China. Palaeogeography, Palaeoclimatology, Palaeoecology 133, 227–242.

Flynn, L., Wu, W.Y., 2001. The late Cenozoic mammal record in North China and the Neogene mammal zonation of Europe. Bolletino della Societa Paleontologica Italiana 40 (2), 195–199 (in Italian).

Forsten, A., 1985. Chinese Turolian Hipparion in the Lagrelius collection. Bulletin of the Geological Institution of the University of Uppsala, New Series 11, 113–124.

Fortelius, M., Eronen, J., Jernvall, J., Liu, L.P., Pushkina, D., Rinne, J., Tesakov, A., Vislobokova, I., Zhang, Z.Q., Zhou, L.P., 2002. Fossil mammals resolve regional patterns of Eurasian climate change over 20 million years. Evolutionary Ecology Research 4, 1005–1016.

Guo, Z.T., Ruddiman, W.F., Hao, Q.Z., Wu, H.B., Qiao, Y.S., Zhu, R.X., Peng, S.Z., Wei, J.J., Yuan, B.Y., Liu, T.S., 2002. Onset of Asian desertification by 22 Myr ago inferred from loess deposits in China. Nature 416, 159–163.

Han, J., Fyfe, W.S., Gu, Z., 2002. Assessment of the palaeoclimate during 3.0–2.6 Ma registered by transition of Red Clay to loess–palaeosol sequence in central North China. Palaeogeography, Palaeoclimatology, Palaeoecology 185, 355–368.

Heller, F., Liu, T.S., 1982. Magnetostratigraphical dating of Chinese loess deposits in China. Nature 300, 431–433.

Heller, F., Liu, T.S., 1986. Paleoclimatic and sedimentary history from magnetic susceptibility of loess in China. Geophysical Research Letters 13, 1169–1171.

Heslop, D., Langereis, C.G., Dekkers, M.J., 2000. A new astronomical timescale for the loess deposits of Northern China. Earth and Planetary Science Letters 184, 125–139.

Hus, J.J., Han, J.M., 1992. The contribution of loess magnetism in China to the retrieval of past global changes-some problems. Physics of the Earth and Planetary Interiors 70, 154–168.
Jokela, T., Eronen, J.T., Kaakinen, A., Liu, L.P., Passey, B., Zhang, Z.Q., Fu, M., 2005. Translation of Otto Zdansky's "The Localities of the *Hipparion* Fauna in Baode County in Northwest Shanxi" (1923). Paleontologia Electronica 8 (1), 3A (10p).
Kaakinen, A., Lunkka, J.P., 2003. Sedimentation of the Late Miocene Bahe Formation and its implications for stable environments adjacent to Qinling mountains in Shaanxi, China. Journal of Asian Earth Sciences 22, 67–78.
Kirschvink, J.L., 1980. The least-squares line and plane and the analysis of paleomagnetic data. Geophysical Journal of the Royal Astronomic Society 62, 699–718.
Kurtén, B., 1952. The Chinese Hipparion fauna. Commentationes Biological, Societas Scientiarum Fennica 13, 1–82.
Li, C.K., Wu, W.Y., Qiu, Z.D., 1984. Chinese Neogene: subdivision and correlation. Vertebrata PalAsiatica 22 (3), 163–178 (in Chinese with English abstract).
Lisiecki, L.E., Raymo, M.E., 2005. A Pliocene–Pleistocene stack of 57 globally distributed benthic $\delta^{18}$O records. Palaeoceanography 20, PA1003. doi:10.1029/2004PA001071.
Liu, T.S., 1985. Loess and the Environment. China Ocean Press, Beijing, p. 215.
Liu, T.S., Ding, Z.L., 1990. Progress of loess research in China (part 2): Paleoclimatology and global change. Quaternary Sciences 1, 1–9 (in Chinese with English abstract).
Liu, T.S., Ding, Z.L., 1998. Chinese loess and the paleomonsoon. Annual Review of Earth and Planetary Sciences 26, 111–145.
Liu, T.S., Li, C.K., Zhai, R.J., 1978. Pliocene vertebrates of Lantian, Shensi. Tertiary mammalian fauna of the Lantian District, Shensi. Professional Papers of Stratigraphy and Paleontology 7, 149–200 (in Chinese with English abstract).
Liu, X.M., Liu, T.S., Xu, T.C., Liu, C., Chen, M.Y., 1988. The primary study on magnetostratigaphy of a loess profile in Xifeng area, Gansu Province. Geophysical Journal of the Royal Astronomical Society 92, 345–348.
Liu, X.M., An, Z.S., Qiang, X.K., 2001. Magnetic properties of the Tertiary red clay from Gansu Province, China and its paleoclimatic significance. Science in China, Series D 44, 635–651.
Mo, D.W., Derbyshire, E., 1991. The depositional environment of the late Pliocene "red clay", Jing-Le Basin, Shanxi Province, China. Sedimentary Geology 70, 33–40.
Nawrocki, J., Bogucki, A., Lanczont, M., Nowaczykd, N.R., 2002. The Matuyama–Brunhes boundary and the nature of magnetic remanence acquisition in the loess–paleosol sequence from the western part of the East European loess province. Palaeogeography, Palaeoclimatology, Palaeoecology 188, 39–50.
Pei, W.Z., Zhou, M.Z., Zheng, J.J., 1963. Chinese Cenozoic Erathem. Science Press, Beijing, pp. 1–31 (in Chinese).
Qiang, X.K., Li, Z.X., Powell, C.McA., Zheng, H.B., 2001. Magnetostratigraphic record of the Late Miocene onset of the East Asian monsoon, and Pliocene uplift of northern Tibet. Earth and Planetary Science Letters 187, 83–93.
Qiu, Z.D., 1988. Neogene micromammals of China. In: Chen, E.K.J. (Ed.), The Paleoenvironment of East Asian from the MidTertiary, II. University of Hong Kong Press, Hong Kong, pp. 834–848.
Qiu, Z.X., Qiu, Z.D., 1990. Neogene local mammalian faunas: succession and ages. Journal of Stratigraphy 14, 241–260 (in Chinese with English abstract).
Qiu, Z.X., Huang, W.L., Guo, Z.H., 1987. The Chinese hipparionine fossils. Palaeontologia Sinica, New Series C 25, 1–250 (in Chinese with English Abstract).
Rutter, N., Ding, Z.L., Evans, M.E., Liu, T.S., 1991. Baoji-type pedostratigraphic section, Loess Plateau, north-central China. Quaternary Science Reviews 10, 11–22.
Sefve, I., 1927. Die Hipparionen Nord-Chinas. Palaeontologia Sinica, Series C 4 (2), 1–94.
Shackleton, N.J., Berger, A., Peltier, W.R., 1990. An alternative astronomical calibration of the lower Pleistocene timescale based on ODP Site 677. Transactions of the Royal Socity of Edinburgh. Earth Sciences 81, 251–261.
Shackleton, N.J., Hall, M.A., Pate, D., 1995. Pliocene stable isotope stratigraphy of ODP Site 846. In: Pisias, G., Mayer, L.A., Janecek, T.R., et al. (Eds.), Proceedings of ODP Science Results, vol. 138, pp. 337–355.
Shi, N., Cao, J.X., Konigsson, L.K., 1993. Late Cenozoic vegetational history and the Pliocene–Pleistocene boundary in the Yushe Basin, S.E. Shanxi, China. Grana 32, 260–271.
Spassov, S., Heller, F., Evans, M.E., Yue, L.P., Ding, Z.L., 2001. The Matuyama/Brunhes geomagnetic polarity transition at Lingtai and Baoji, Chinese Loess Plateau. Physics and Chemistry of the Earth (A) 26, 899–904.
Sun, D.H., An, Z.S., Shaw, J., Bloemendal, J., Sun, Y.B., 1998. Magnetostratigraphy and paleoclimatic significance of Late Tertiary aeolian sequences in the Chinese Loess Plateau. Geophysical Journal International 134, 207–212.
Sun, Y.B., Clemens, S.C., An, Z.S., Yu, Z.W., 2006. Astronomical timescale and palaeoclimatic implication of stacked 3.6-Myr monsoon records from the Chinese Loess Plateau. Quaternary Science Reviews 25, 33–48.
Tedford, R.H., Flynn, L.J., Qiu, Z.X., Opdyke, N.D., Downs, W.R., 1991. Yushe Basin, China: paleomagnetically calibrated mammalian biostratigraphic standard for the Late Neogene of Eastern Asia. Journal of Vertebrate Paleontology 11, 519–526.
Teilhard, D.C., Young, C.C., 1930. Some correlations between the geology of China proper and geology of Mongolia. Bulletin of the Geological Society of China 9 (2), 119–125.
Teilhard, D.C., Young, C.C., 1931. Fossils mammals from the Late Cenozoic of Northern China. Palaeontologia Sinica, Series C 9 (1), 1–67.
Wang, W.M., Deng, T., 2005. A general introduction to recent advance in Neogene studies. Journal of Stratigraphy 29, 104–108 (in Chinese with English abstract).
Wang, L., Lu, H.Y., Wu, N.Q., Li, J., Pei, Y.P., Tong, G.B., Peng, S.Z., 2006. Palynological evidence for Late Miocene–Pliocene vegetation evolution recorded in the red clay sequence of the central Chinese Loess Plateau and implication for Palaeoenvironmental change. Palaeogeography, Palaeoclimatology, Palaeoecology 241, 118–128.
Wu, N.Q., Pei, Y.P., Lu, H.Y., Guo, Z.T., Li, F.J., Liu, T.S., 2006. Marked ecological shifts during 6.2–2.4 Ma revealed by a terrestrial molluscan record from the Chinese Red Clay Formation and implication for palaeoclimatic evolution. Palaeogeography, Palaeoclimatology, Palaeoecology 223, 287–299.
Xue, X.X., Zhang, Y.X., Yue, L.P., 1995. Discovery and chronological division of the Hipparion fauna in Laogaochuan Village, Fugu County, Shannxi. Chinese Science Bulletin 40, 926–929.
Xue, X.X., Yue, L.P., Wang, J.Q., 2001. Discussion on the Neogene–Quaternary boundary-based on the Xiaqiang Upper Cenozoic profile of Xunyi County, Shaanxi Province. Journal of Stratigraphy 25, 161–165 (in Chinese with English abstract).
Xue, X.X., Zhang, Y.X., Yue, L.P., 2006. Paleoenvironments indicated by the fossil mammalian assemblages from red clay-Loess sequence in the Chinese Loess Plateau since 8.0 Ma B.P. Science in China, Series D 49 (5), 518–530.
Yang, S.L., Hou, S.S., Wang, X., 2000. Completeness and continuity of the Late Tertiary red clay sequence in northern China: evidence from the correlation of magnetostratigraphy and pedostratigraphy between Jingchuan and Lingtai. Quaternary Sciences 20, 435–446 (in Chinese with English abstract).
Yue, L.P., Zhang, Y.X., 1998. Hipparion fauna and magnetostratigraphy in Hefeng, Jingle, Shanxi Province. Vertenrata PalAsiatica 36, 76–80 (in Chinese with English abstract).
Yue, L.P., Deng, T., Zhang, Y.X., Wang, J.Q., Zhang, R., Yang, L.R., Heller, F., 2004. Magnetostratigraphy of stratotype section of the Baode Stage. Journal of Stratigraphy 28, 48–63 (in Chinese with English abstract).
Zdansky, O., 1923. Fundorte der Hipparion–Fauna um Pao-Te-Hsien in NW-Shansi. Bulletin of the Geological Survey of China 5, 69–81.
Zdansky, O., 1924. Jungtertiare Carnivoren Chinas. Palaeontologia Sinica, Series C 2 (1), 1–150.
Zhang, Z.Q., 2006. Chinese Late Neogene land mammal community and the environmental changes of East Asia. Vertebrata PalAsiatica 44, 133–142 (in Chinese with English abstract).
Zhang, Z.Q., Liu, L.P., 2005. The Late Neogene mammal biochronology in the Loess Plateau, China. Annales de Paleontologie 91, 257–266.
Zhang, Y.X., Xue, X.X., Yue, L.P., 1995. Age and division of Neogene "Red Bed" of Laogaochuan, Fugu County, Shaanxi. Journal of Stratigraphy 19, 214–219 (in Chinese with English abstract).
Zhang, Y.X., Yue, L.P., Chen, D.L., Xue, X.X., 1997. Petrographic marks for stratigraphic division of the Neogene Red Clay in North China and their significance. Journal of Stratigraphy 21, 63–67 (in Chinese with English abstract).
Zhang, Y.X., Yue, L.P., Xue, X.X., 1999. The division and correlation of the Upper Neogene Jingle Red Clay of in Shaanxi and Shanxi. Journal of Stratigraphy 23, 310–315 (in Chinese with English abstract).
Zhang, Y.X., Yue, L.P., Cao, H.X., 2001. The ecological sequence of Hipparion fauna in the middle reaches of the Yellow River during Neogene. Chinese Science Bulletin 46, 1196–1199 (in Chinese).
Zhang, Z.Q., Gentry, A.W., Kaakinen, A., Liu, L.P., Lunkka, J.P., Qiu, Z.D., Sen, S., Scott, R., Werdelin, L., Zheng, S.H., Fortelius, M., 2002. Land mammal faunal sequence of the Late Miocene of China: new evidence from Lantian, Shaanxi Province. Vertenrata PalAsiatica 40, 165–176 (in Chinese with English abstract).
Zhao, J.B., 1989. The study of the red soil of Neogene in Xi'an and Baode of Shanxi. Acta Sedimentologica Sinica 7, 113–120 (in Chinese with English abstract).
Zheng, H.B., An, Z.S., Shaw, J., 1992. New contributions to Chinese Plio-Pleistocene magnetostratigraphy. Physics of the Earth and Planetary Interiors 70, 146–153.
Zhou, L.P., Shackleton, N.J., 1999. Misleading positions of geomagnetic reversal boundaries in Eurasian loess and implications for correlation between continental and marine sedimentary sequences. Earth and Planetary Science Letters 168, 117–130.
Zhou, L.P., Oldfield, F., Wintle, A.G., Robinson, S.G., Wang, J.T., 1990. Partly pedogenic origin of magnetic variations in Chinese loess. Nature 346, 737–739.
Zhou, L.P., Shackleton, N.J., Dodonov, A.E., 2000. Stratigraphical interpretation of geomagnetic polarity boundaries in Eurasian loess. Quaternary Sciences 20, 196–202 (in Chinese with English abstract).
Zhu, R.X., Guo, B., Ding, Z.L., Guo, Z.T., Kazansky, A., Matasova, G., 2000. Gauss–Matuyama polarity transition obtained from a loess section at Weinan, north-central China. Journal of Geophysical Research 43, 654–671 (in Chinese with English abstract).